Hindawi
Advances in High Energy Physics
Volume 2018, Article ID 5961031, 12 pages
https://doi.org/10.1155/2018/5961031

Research Article

S-Wave Heavy Quarkonium Spectra: Mass, Decays, and Transitions

Halil Mutuk

Physics Department, Faculty of Arts and Sciences, Ondokuz Mayis University, 55139 Samsun, Turkey

Correspondence should be addressed to Halil Mutuk; halilmutuk@gmail.com

Received 20 August 2018; Revised 18 October 2018; Accepted 30 October 2018; Published 25 November 2018

Guest Editor: Xian-Wei Kang

In this paper we revisited phenomenological potentials. We studied S-wave heavy quarkonium spectra by two potential models. The first one is power potential and the second one is logarithmic potential. We calculated spin averaged masses, hyperfine splittings, Regge trajectories of pseudoscalar and vector mesons, decay constants, leptonic decay widths, two-photon and two-gluon decay widths, and some allowed M1 transitions. We studied ground and 4 radially excited S-wave charmonium and bottomonium states via solving nonrelativistic Schrödinger equation. Although the potentials which were studied in this paper are not directly QCD motivated potential, obtained results agree well with experimental data and other theoretical studies.

1. Introduction

Heavy quarkonium is the bound state of $b\bar{b}$ and $c\bar{c}$ and one of the most important playgrounds for our understanding of the strong interactions of quarks and gluons. Quantum chromodynamics (QCD) is thought to be the *true* theory of these strong interactions. QCD is a nonabelian local gauge field theory with the symmetry group $SU(3)$. In principle, one should be able to calculate hadronic properties such as mass spectrum and transitions by using QCD principles. But QCD does not readily supply us these hadronic properties. This challenge can be attributed to the several features that are not present in other local gauge field theories.

Foremost, being a nonabelian gauge theory, gluons which are gauge bosons, have color charge and interact among themselves. Unlike from quantum electrodynamics (QED), where a photon does not interact with other photon, in QCD one must consider interactions among gluons. This nonabelian nature of the theory makes some calculations complicated, for example, loops in propagators.

There are three other important features of QCD: *asymptotic freedom*, *confinement,* and *dynamical breaking of chiral symmetry*. Asymptotic freedom says that strong interaction coupling constant, α_s, is a function of momentum transfer. When the momentum transfer in a quark-quark collision increases (at short distances), the coupling constant becomes weaker whereas it becomes larger when momentum transfer decreases (at large distances). The idea behind confinement is that, there are no free quarks outside of a hadron; i.e., color charged particles (quarks and gluons) cannot be isolated out of hadrons. Flux tube model gives a reasonable explanation of confinement. When the distance between quark-antiquark (or quarks) pair increases, the gluon field between a pair of color charges forms a flux tube (or string) between them resulting a potential energy which depends linearly on the distance, $V(r) =\sim \sigma r$ where σ is the string constant. As distance increases between quarks, the potential energy can create new quark-antiquark pairs in colorless forms instead of a free quark. Up to now, nobody has been able to prove that confinement from QCD. Lattice QCD calculations simulate this confinement well and give a value for the string tension [1]. The last feature of QCD is the dynamical breaking of chiral symmetry. The QCD Lagrangian with N quark flavor has an exact chiral $SU(N) \times SU(N)$ symmetry but breaks down to $SU(N)$ symmetry because of the nonvanishing expectation value of QCD vacuum [2, 3]. The Goldstone bosons corresponding to this symmetry breaking are the pseudoscalar mesons.

The present aspects of the QCD caused other approaches to deal with these challenges. QCD sum rules, Lattice QCD,

and potential models (quark models) are examples of these approaches. These approaches are nonperturbative since the strong interaction coupling constant, which should be the perturbation parameter of QCD is of the order one in low energies, hence the truncation of the perturbative expansion cannot be carried out. Since perturbation theory is not applicable, a nonperturbative approach has to be used to study systems that involve strong interactions. QCD sum rules and lattice QCD are based on QCD itself whereas in potential models, one assumes an interquark potential and solves a Schrödinger-like equation. The advantage of potential model is that, excited states can be studied in the framework of potential models whereas in QCD sum rules and lattice QCD, only the ground state or in some exceptional cases excited states can be studied.

After the discovery of charmonium ($c\overline{c}$) states, potential models have played a key role in understanding of heavy quarkonium spectroscopy [4, 5]. These potentials were in type of Coulomb plus linear confining potential with spin dependent interactions. The discovery of bottomonium ($b\overline{b}$) states were well described by the potential model picture which was used in the charmonium case. Heavy quarkonium spectroscopy was studied since that era with fruitful works [6–18]. A general review about potential models can be found in [19, 20] and references therein.

In the potential models, many features such as mass spectra and decay properties of heavy quarkonium could be described by an interquark potential in two-body Schrödinger equation. Interquark potentials are obtained both from phenomenology and theory. In the phenomenological method, it is assumed that a potential exist with some parameters to be determined by fits to the data. In the theory side, one can use perturbative QCD to determine the potential form at short distances and use lattice QCD at long distances [19]. These potentials can be classified as QCD motivated potentials [21–25] and phenomenological potentials [26–31]. The most commonly used phenomenological potentials are power-law potentials, for example [26] and logarithmic potentials, for example [30]. The detailed properties of these type potentials are studied extensively in [29]. All the potentials which are mentioned here have almost similar behaviour in the range of $0.1\ \text{fm} \leq r \leq 1\ \text{fm}$ which is characteristic region of charmonium and bottomonium systems [32, 33]. Outside the range, the behaviour of potentials differ. Up to now, no one was able to obtain a potential which is compatible at the whole range of distances by using QCD principles.

The potential model calculations have been quite successful in describing the hadron spectrum. Most of the phenomenological potentials must satisfy the following conditions:

$$\frac{dV}{dr} > 0, \qquad \frac{d^2V}{dr^2} \leq 0. \tag{1}$$

It means that static potential is a monotone nondecreasing and concave function of r which is a general property of gauge theories [34].

The great success of quarkonium phenomenology was somehow cracked at 2003 after the observation of $X(3872)$ [35]. The properties of this exotic particle are not compatible with the conventional quark model, the reason why it is named *exotic*. For example in [36], the authors studied $X(3872)$ near threshold zero in the $D^0\overline{D}^{*0}$ S-wave. There are other exotic states, XYZ, and the exotic particle zoo is growing. In this paper we will present some exotic states in the framework of quark model.

Energy spectra of heavy quarkonium are a rich source of the information on the nature of interquark forces and decay mechanisms. The prediction of mass spectrum in accordance with the experimental data does not verify the validity of a model for explaining hadronic interactions. Different potentials can produce reliable spectra with the experimental data. Thus other physical properties such as decay constants, leptonic decay widths, radiative decay widths, etc. need to be calculated.

A specific form of the QCD potential in the whole range of distances is not known. Therefore one needs to use potential models. In this work we revisited a power-law potential [26] and a logarithmic potential [30] to study S-wave heavy quarkonium. These potentials satisfy Eqn. (1), i.e. having nonsingular behaviour for $r \longrightarrow 0$. For our purposes, it must be mentioned that power-law and logarithmic potentials have nice scaling properties when used with a nonrelativistic Schrödinger equation [19]. We generated S-wave charmonium and bottomonium mass spectrum with the decays and M1 transitions. At Section 2 we give out theoretical model. In Sections 3 and 4, we generate S-wave heavy quarkonium spectrum, decays and transitions. In Section 5 we discuss our results and in Section 6 we conclude our results.

2. Formulation of the Model

When quark model was proposed, many authors treated baryons in detail with the harmonic oscillator quark model by using harmonic oscillator wave functions [37–39]. Mesons comparing to baryons are simpler objects since they are composites of two quarks. The reason for using harmonic oscillator wave function is that they form a complete set for a confining potential [40].

In order to obtain mass spectra, we solved Schrödinger equation by variational method. The variational method by using harmonic oscillator wave function gave successful results for heavy and light meson spectrum [15, 41, 42]. The procedure for this method is calculating expectation value of the Hamiltonian via the trial wave function:

$$E = \frac{\langle \Psi | H | \Psi \rangle}{\langle \Psi | \Psi \rangle}. \tag{2}$$

The mass of the meson is found by adding two times the mass of quark to the eigenenergy

$$M = 2m_q + E. \tag{3}$$

The Hamiltonian we consider is

$$H = M + \frac{p^2}{2\mu} + V(r) \tag{4}$$

Table 1: Spin-averaged mass spectrum of charmonium (in MeV).

State	Power	Logarithmic	[15]	[12]
1S	3067	3067	3067	3117
2S	3701	3655	3667	3684
3S	4054	3980	4121	4078
4S	4306	4204	4513	4407
5S	4504	4376	4866	

where $M = m_q + m_{\overline{q}}$, p is the relative momentum, μ is the reduced mass, and $V(r)$ is the potential between quarks. The spectrum can be obtained via solving Schrödinger equation

$$H\left|\Psi_n\right\rangle = E_n\left|\Psi_n\right\rangle \tag{5}$$

with the harmonic oscillator wave function defined as

$$\Psi_{nlm}(r,\theta,\phi) = R_{nl}(r)\,Y_{lm}(\theta,\phi). \tag{6}$$

Here R_{nl} is the radial wave function given as

$$R_{nl} = N_{nl} r^l e^{-\nu r^2} L^{l+1/2}_{(n-l)/2}\left(2\nu r^2\right) \tag{7}$$

with the associated Laguerre polynomials $L^{l+1/2}_{(n-l)/2}$ and the normalization constant

$$N_{nl} = \sqrt{\sqrt{\frac{2\nu^3}{\pi}}\frac{2\left((n-l)/2\right)!\nu^l}{\left((n+l)/2+1\right)!!}}. \tag{8}$$

$Y_{lm}(\theta,\phi)$ is the well-known spherical harmonics.

Armed with these, the expectation value of the given Hamiltonian can be calculated. In the variational method, one chooses a trial wave function depending on one or more parameters and then finds the values of these parameters by minimizing the expectation value of the Hamiltonian. It is a good tool for finding ground state energies but as well as energies of excited states. The condition for obtaining excited states energies is that the trial wave function should be orthogonal to all the energy eigenfunctions corresponding to states having a lower energy than the energy level considered. In (7), ν is treated as a variational parameter and it is determined for each state by minimizing the expectation value of the Hamiltonian.

In the following sections we study power-law and logarithmic potentials in order to obtain full spectrum.

3. Mass Spectra of Power-Law and Logarithmic Potentials

Power-law potential is given by [26]

$$V(r) = -8.064\ \text{GeV} + 6.898\ \text{GeV}\ r^{0.1}. \tag{9}$$

They showed that upsilon and charmonium spectra can be fitted with that potential. The small power of r refers to a situation in which the spacing of energy levels is independent of the quark masses. This situation is also valid for the purely logarithmic potential [30]

$$V(r) = -0.6635\ \text{GeV} + 0.733\ \text{GeV}\ \ln\left(r \times 1\ \text{GeV}\right). \tag{10}$$

At first step we obtained spin averaged mass spectrum for $c\overline{c}$ and $b\overline{b}$ systems, respectively. The constituent quark masses are $m_c = 1.8$ GeV and $m_b = 5.174$ GeV for power-law potential and $m_c = 1.5$ GeV and $m_b = 4.906$ GeV for logarithmic potential. Table 1 shows the charmonium spectrum and Table 2 shows the bottomonium spectrum.

Since the interquark potential does not contain the spin dependent part, (2) gives the spin averaged mass for the corresponding states. The calculated masses agree well with the available experimental data and with the values obtained from other theoretical studies. A general potential usually includes spin-spin interaction, spin-orbit interaction, and tensor force terms. To obtain whole picture, it is necessary to consider spin dependent terms within the potential. For $l \geq 1$, there are spin-orbit and tensor force terms which contribute to the fine structure. For equal mass m, the spin-orbit interaction is given by

$$V_{SO} = 2\frac{\alpha_s}{m_q^2 r^3}\left(3\left(\mathbf{S_1}+\mathbf{S_2}\right)\cdot\mathbf{L}\right) \tag{11}$$

and is responsible for the P wave splittings. Again for equal mass m, the tensor potential is given by

$$V_T = \frac{4}{3}\frac{\alpha_s}{m_q^2 r^3}\left(\frac{3\left(\mathbf{S_1}\cdot\mathbf{r}\right)\left(\mathbf{S_2}\cdot\mathbf{r}\right)}{r^2} - \mathbf{S_1}\cdot\mathbf{S_2}\right). \tag{12}$$

For $l = 0$, there is spin-spin term which we will consider in the present work. In the model of the spin averaged mass spectra discussion, all the spin dependent effects are ignored and hence it fails to take into account the splittings due to spin. For example, such splitting exist between the $\eta_c(1S)$ and J/ψ mesons by $\Delta m \simeq 110$ MeV. These mesons occupy the $l = 0$ level. The $c\overline{c}$ in the $\eta_c(1S)$ have $s = 0$, while in the J/ψ, $s = 1$. As a result of this, the mass difference should be related to spin dependent interaction.

3.1. Spin-Spin Interaction. Mass splitting is closely connected with the Lorentz-structure of the quark potential [45]. The origin of the spin-spin interaction term lies in the one-gluon exchange term which is related to $1/r$. Spin is proportional of the magnetic moment of a particle. Magnetic moments generate short range fields $\sim 1/r^3$. In the case of heavy quarkonium systems which are nonrelativistic, wave functions of two particles overlap in a significant amount. This means that particles are very close to each other. So spin-spin

Table 2: Spin-averaged mass spectrum of Bottomonium (in MeV).

State	Power	Logarithmic	[15]	[12]
1S	9473	9444	9443	9523
2S	10049	10033	9729	10035
3S	10384	10357	10312	10373
4S	10624	10581	10593	
5S	10813	10753	10840	
6S	10986	10964	11065	

Table 3: Charmonium mass spectrum (in MeV). In [18] LP denotes linear potential and SP denotes screened potential.

State	Exp. [43]	Power	Logarithmic	[13]	[11]	[18] LP	[18] SP
$\eta_c(1S)$	2984	2980	2954	2979	2982	2983	2984
$\eta_c(2S)$	3639	3624	3555	3623	3630	3635	3637
$\eta_c(3S)$		3983	3887	3991	4043	4048	4004
$\eta_c(4S)$		4240	4117	4250	4384	4388	4264
$\eta_c(5S)$		4441	4294	4446		4690	4459
J/ψ	3097	3096	3104	3097	3090	3097	3097
$\psi(2S)$	3686	3727	3689	3673	3672	3679	3679
$\psi(3S)$	4040	4078	4011	4022	4072	4078	4030
$\psi(4S)$		4328	4233	4273	4406	4412	4281
$\psi(5S)$		4525	4403	4463		4711	4472

interactions play a significant role in the dynamics. The *spin-spin* interaction term of two particles can be written as

$$V_{SS}(r) = \frac{32\pi\alpha_s}{9m_q m_{\overline{q}}} \mathbf{S_q} \cdot \mathbf{S_{\overline{q}}} \delta(\mathbf{r}). \tag{13}$$

This term can explain s wave splittings and has no contribution to $l \neq 0$ states. Putting this term into Schrödinger equation we get

$$E_{HF} = \frac{32\pi\alpha_s}{9m_q m_{\overline{q}}} \int d^3 r \Psi^{\star}(\mathbf{r}) \boldsymbol{\Psi}(\mathbf{r}) \delta(\mathbf{r}) \left\langle \mathbf{S_q} \cdot \mathbf{S_{\overline{q}}} \right\rangle. \tag{14}$$

Implementing Dirac-delta function property

$$\int f(x) \delta(x) dx = f(0), \tag{15}$$

we obtain

$$E_{HF} = \frac{32\pi\alpha_s}{9m_q m_{\overline{q}}} |\Psi(0)|^2 \left\langle \mathbf{S_q} \cdot \mathbf{S_{\overline{q}}} \right\rangle. \tag{16}$$

The matrix element of spin products can be obtained via

$$\mathbf{S}_1 \cdot \mathbf{S}_2 = \frac{1}{2}\left(\mathbf{S}^2 - \mathbf{S}_1^2 - \mathbf{S}_2^2\right) = \frac{1}{2}\left(S(S+1) - \frac{3}{2}\right) \tag{17}$$

so that

$$\left\langle \mathbf{S_q} \cdot \mathbf{S_{\overline{q}}} \right\rangle = \begin{cases} \frac{1}{4}, & \text{for } \overrightarrow{S} = 1 \\ -\frac{3}{4}, & \text{for } \overrightarrow{S} = 0. \end{cases} \tag{18}$$

Therefore we obtain hyperfine splittings energy as

$$E_{HF} = \begin{cases} \frac{8\pi\alpha_s}{9m_q m_{\overline{q}}} |\Psi(0)|^2, & \text{for } \overrightarrow{S} = 1 \\ -\frac{8\pi\alpha_s}{3m_q m_{\overline{q}}} |\Psi(0)|^2, & \text{for } \overrightarrow{S} = 0. \end{cases} \tag{19}$$

Here $\Psi(0)$ is the wave function at the origin and can be obtained by the following relation:

$$|\Psi(0)|^2 = \frac{\mu}{2\pi\hbar} \left\langle \frac{dV(r)}{dr} \right\rangle. \tag{20}$$

Expectation value is obtained by the wave function given in (6). S-wave charmonium and bottomonium masses can be seen in Tables 3 and 4. In this calculation, α_s is taken to be 0.37 for charmonium and 0.26 for bottomonium [15].

The mass differences are shown in Tables 5 and 6 for charmonium and bottomonium, respectively.

As can be seen from Tables 3, 4, 5, and 6 our results are compatible with both experimental and theoretical results.

The Regge trajectories for pseudoscalar and vector mesons are shown in Figures 1 and 2 for charmonium and in Figures 3 and 4 for bottomonium.

As can be seen from figures, Regge trajectories show nonlinear behaviour.

4. Dynamical Properties

4.1. Decay Constants. Leptonic decay constants give information about short distance structure of hadrons. In the experiments this regime is testable since the momentum transfer is very large. The pseudoscalar (f_p) and the vector

Table 4: Bottomonium mass spectrum (in MeV).

State	Exp. [43]	Power	Logarithmic	[14]	[18]	[44]	[16]
$\eta_b(1S)$	9399	9452	9420	9389	9390	9402	9455
$\eta_b(2S)$	9999	10030	10011	9987	9990	9976	9990
$\eta_b(3S)$		10367	10338	10330	10326	10336	10330
$\eta_b(4S)$		10608	10562	10595	10584	10623	
$\eta_b(5S)$		10798	10735	10817	10800	10869	
$\eta_b(6S)$		11005	10990	11011	10988	11097	
$\Upsilon(1S)$	9460	9480	9452	9460	9460	9465	9502
$\Upsilon(2S)$	10023	10055	10040	10016	10015	10003	10015
$\Upsilon(3S)$	10355	10393	10364	10351	10343	10354	10349
$\Upsilon(4S)$	10579	10629	10588	10611	10597	10635	10607
$\Upsilon(5S)$	10865	10818	10759	10831	10811	10878	10818
$\Upsilon(6S)$	11019	11019	11006	11023	10997	11102	10995

Table 5: Mass differences of S-wave charmonium states (in MeV).

State	Exp. [43]	Power	Logarithmic	[13]	[11]	[18] LP	[18] SP
J/ψ-$\eta_c(1S)$	113	116	150	118	108	114	113
$\psi(2S)$-$\eta_c(2S)$	47	103	134	50	42	44	42
$\psi(3S)$-$\eta_c(3S)$		95	124	31	29	30	26
$\psi(4S)$-$\eta_c(4S)$		88	116	23	22	24	17
$\psi(5S)$ - $\eta_c(5S)$		84	109	17		21	13

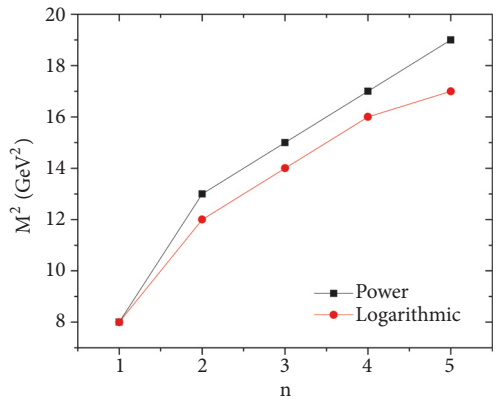

Figure 1: Regge trajectories of pseudoscalar charmonium in (n, M^2) plane. The polynomial fit is $M^2 = -0.397857\ n^2 + 5.04014\ n + 4.356$ (GeV^2) for power potential and $M^2 = -0.382143\ n^2 + 4.65786\ n + 4.55$ (GeV^2) for logarithmic potential.

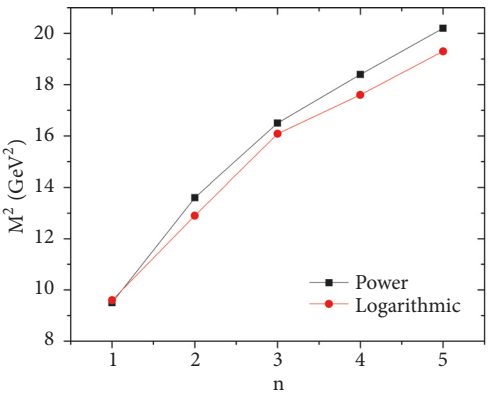

Figure 2: Regge trajectories of vector charmonium in (n, M^2) plane. The polynomial fit is $M^2 = -0.405\ n^2 + 5.091\ n + 4.986$ (GeV^2) for power potential and $M^2 = -0.403571\ n^2 + 4.80643\ n + 5.316$ (GeV^2) for logarithmic potential.

(f_v) decay constants are defined, respectively, through the matrix elements [12]

$$p^\mu f_p = i \left\langle 0 \left| \overline{\Psi} \gamma^\mu \gamma^5 \Psi \right| p \right\rangle \tag{21}$$

and

$$m_v f_v \epsilon^\mu = \left\langle 0 \left| \overline{\Psi} \gamma^\mu \Psi \right| v \right\rangle . \tag{22}$$

In the first relation, p^μ is meson momentum and $|p\rangle$ is pseudoscalar meson state. In the second relation, m_v is mass, ϵ^μ is the polarization vector, and $|v\rangle$ is the state vector of meson.

The matrix elements can be calculated by quark model wave function in the momentum space. The result is

$$f_p = \sqrt{\frac{3}{m_p}} \int \frac{d^3k}{(2\pi)^3} \sqrt{1 + \frac{m_q}{E_k}} \sqrt{1 + \frac{m_{\overline{q}}}{E_{\overline{k}}}} \left(1 - \frac{k^2}{\left(E_k + m_q\right)\left(E_{\overline{k}} + m_{\overline{q}}\right)} \right) \phi\left(\vec{k}\right) \tag{23}$$

Table 6: Mass differences of S-wave bottomonium states (in MeV).

State	Exp. [43]	Power	Log	[14]	[18]	[44]	[16]
$\Upsilon(1S)$-$\eta_b(1S)$	61	28	32	71	70	63	47
$\Upsilon(2S)$-$\eta_b(2S)$	24	25	29	29	25	27	25
$\Upsilon(3S)$-$\eta_b(3S)$		26	26	21	17	18	19
$\Upsilon(4S)$-$\eta_b(4S)$		21	26	16	13	12	
$\Upsilon(5S)$-$\eta_b(5S)$		20	24	14	11	9	
$\Upsilon(6S)$-$\eta_b(6S)$	14	16	12	9			

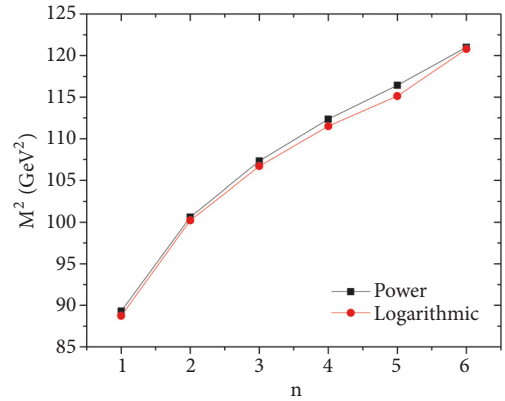

Figure 3: Regge trajectories of pseudoscalar bottomonium in (n, M^2) plane. The polynomial fit is $M^2 = -0.79\ n^2 + 11.5586\ n + 79.36\ (GeV^2)$ for power potential and $M^2 = -0.636071\ n^2 + 10.3054\ n + 80.92\ (GeV^2)$ for logarithmic potential.

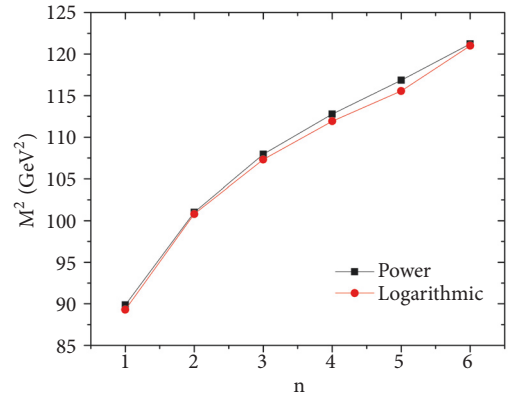

Figure 4: Regge trajectories of vector bottomonium in (n, M^2) plane. The polynomial fit is $M^2 = -0.809286\ n^2 + 11.6401\ n + 79.812\ (GeV^2)$ for power potential and $M^2 = -0.7475\ n^2 + 11.1579\ n + 79.936\ (GeV^2)$ for logarithmic potential.

for pseudoscalar meson and

$$f_v = \sqrt{\frac{3}{m_v}} \int \frac{d^3k}{(2\pi)^3} \sqrt{1 + \frac{m_q}{E_k}} \sqrt{1 + \frac{m_{\overline{q}}}{E_{\overline{k}}}} \left(1 + \frac{k^2}{3\left(E_k + m_q\right)\left(E_{\overline{k}} + m_{\overline{q}}\right)}\right) \phi\left(\vec{k}\right) \tag{24}$$

for the vector meson [12].

In the nonrelativistic limit, these two equations take a simple form which is known to be Van Royen and Weisskopf relation [46] for the meson decay constants

$$f_{p/v}^2 = \frac{12\left|\Psi_{p/v}(0)\right|^2}{m_{p/v}}. \tag{25}$$

The first-order correction which is also known as QCD correction factor is given by

$$\overline{f}_{p/v}^2 = \frac{12\left|\Psi_{p/v}(0)\right|^2}{m_{p/v}} C^2(\alpha_s) \tag{26}$$

where $C(\alpha_s)$ is given by [47]

$$C(\alpha_s) = 1 - \frac{\alpha_s}{\pi}\left(\Delta_{p/v} - \frac{m_q - m_{\overline{q}}}{m_q + m_{\overline{q}}} \ln \frac{m_q}{m_{\overline{q}}}\right). \tag{27}$$

Here $\Delta_p = 2$ for pseudoscalar mesons and $\Delta_v = 8/3$ for vector mesons. Decay constants are given in Tables 7 and 8 for pseudoscalar and vector mesons, respectively.

4.2. Leptonic Decay Widths. Leptonic decay of a vector meson with $J^{PC} = 1^{--}$ quantum numbers can be pictured by the following annihilation via a virtual photon

$$V\left(q\overline{q}\right) \longrightarrow \gamma \longrightarrow e^+e^-. \tag{28}$$

This state is neutral and in principle can decay into a different lepton pair rather than electron-positron pair. The above amplitude can be calculated by the Van Royen and Weisskopf relation [46]

$$\Gamma\left(n^3S_1 \longrightarrow e^+e^-\right) = \frac{16\pi\alpha^2 e_q^2 \left|\Psi(0)\right|^2}{m_n^2} \times \left(1 - \frac{16\alpha_s}{3\pi} + \cdots\right), \tag{29}$$

where $\alpha = 1/137$ is the fine structure constant, e_q is the quark charge, m_n is the mass of n^3S_1 state, and $|\Psi_{p/v}(0)|$ is the wave function at the origin of initial state. The term in the parenthesis is the first-order QCD correction factor while $\cdots$ represents higher corrections. The obtained values for leptonic decay widths can be found in Tables 9 and 10 for charmonium and bottomonium, respectively.

Table 7: Pseudoscalar decay constants (in MeV).

State	Exp. [43]	Power f_p	Power $\overline{f_p}$	Logarithmic f_p	Logarithmic $\overline{f_p}$	[15] f_p	[15] $\overline{f_p}$	[12]
$\eta_c(1S)$	335 ± 75	543	415	578	442	471	360	402
$\eta_c(2S)$		473	362	497	380	374	286	240
$\eta_c(3S)$		330	252	442	338	332	254	193
$\eta_c(4S)$		325	248	412	315	312	239	
$\eta_c(5S)$		253	193	387	304			
$\eta_b(1S)$		517	431	585	488	834	694	599
$\eta_b(2S)$		479	400	535	447	567	472	411
$\eta_b(3S)$		345	288	504	421	508	422	354
$\eta_b(4S)$		313	261	482	402	481	401	
$\eta_b(5S)$		283	236	465	388			
$\eta_b(6S)$		208	186	434	374			

Table 8: Vector decay constants (in MeV).

State	Exp. [43]	Power f_v	Power $\overline{f_v}$	Logarithmic f_v	Logarithmic $\overline{f_v}$	[15] f_p	[15] $\overline{f_p}$	[12]
J/ψ	335 ± 75	529	363	563	386	462	317	393
$\psi(2S)$	279 ± 8	463	318	487	334	369	253	293
$\psi(3S)$	174 ± 18	324	222	436	299	329	226	258
$\psi(4S)$		319	219	406	279	310	212	
$\psi(5S)$		248	170	382	262	290	199	
$\Upsilon(1S)$	708 ± 8	516	402	584	455	831	645	665
$\Upsilon(2S)$	482 ± 10	482	373	535	416	566	439	475
$\Upsilon(3S)$	346 ± 50	350	269	504	393	507	393	418
$\Upsilon(4S)$	325 ± 60	316	243	482	375	481	373	388
$\Upsilon(5S)$	369 ± 93	285	222	464	362	458	356	367
$\Upsilon(6S)$		241	203	442	354	439	341	

Table 9: Charmonium leptonic decay widths (in keV). The widths calculated with and without QCD corrections are denoted by $\Gamma_{l^+l^-}$ and $\Gamma^0_{l^+l^-}$.

	Power		Logarithmic		[13]		[15]		Exp. [43]
State	$\Gamma^0_{l^+l^-}$	$\Gamma_{l^+l^-}$	$\Gamma^0_{l^+l^-}$	$\Gamma_{l^+l^-}$	$\Gamma^0_{l^+l^-}$	$\Gamma_{l^+l^-}$	$\Gamma^0_{l^+l^-}$	$\Gamma_{l^+l^-}$	
J/ψ	3.435	1.277	3.154	1.173	11.8	6.60	6.847	2.536	$5.55 \pm 0.14 \pm 0.02$
$\psi(2S)$	2.880	1.071	2.362	0.878	4.29	2.40	3.666	1.358	2.33 ± 0.07
$\psi(3S)$	2.153	0.800	1.888	0.702	2.53	1.42	2.597	0.962	0.86 ± 0.07
$\psi(4S)$	1.839	0.684	1.642	0.610	1.73	0.97	2.101	0.778	0.58 ± 0.07
$\psi(5S)$	1.590	0.591	1.551	0.576	1.25	0.70	1.710	0.633	

Table 10: Bottomonium leptonic decay widths (in keV). The widths calculated with and without QCD corrections are denoted by $\Gamma_{l^+l^-}$ and $\Gamma^0_{l^+l^-}$.

	Power		Logarithmic		[25]		[15]		Exp. [43]
State	$\Gamma^0_{l^+l^-}$	$\Gamma_{l^+l^-}$	$\Gamma^0_{l^+l^-}$	$\Gamma_{l^+l^-}$	$\Gamma^0_{l^+l^-}$	$\Gamma_{l^+l^-}$	$\Gamma^0_{l^+l^-}$	$\Gamma_{l^+l^-}$	
$\Upsilon(1S)$	0.817	0.456	0.847	0.473	2.31	1.60	1.809	0.998	1.340 ± 0.018
$\Upsilon(2S)$	0.686	0.383	0.709	0.396	0.92	0.64	0.797	0.439	0.612 ± 0.011
$\Upsilon(3S)$	0.610	0.340	0.630	0.352	0.64	0.44	0.618	0.341	0.443 ± 0.008
$\Upsilon(4S)$	0.557	0.311	0.576	0.322	0.51	0.35	0.541	0.298	0.272 ± 0.029
$\Upsilon(5S)$	0.526	0.294	0.535	0.299	0.42	0.29	0.481	0.265	0.31 ± 0.07
$\Upsilon(6S)$	0.492	0.278	0.501	0.282	0.31	0.22	0.432	0.238	0.130 ± 0.030

4.3. Two-Photon Decay Width. $^1S_0$ states with $J^{PC} = 0^{-+}$ quantum number of charmonium and bottomonium can decay into two photons. In the nonrelativistic limit, the decay width for $^1S_0$ state can be written as [48]

$$\Gamma\left(^1S_0 \longrightarrow \gamma\gamma\right) = \frac{12\pi\alpha^2 e_q^4 |\Psi(0)|^2}{m_q^2} \times \left(1 - \frac{3.4\alpha_s}{\pi}\right). \quad (30)$$

The term in the parenthesis is the first-order QCD radiative correction. The results are listed in Table 11.

4.4. Two-Gluon Decay Width. Two-gluon decay width is given by [48]

$$\Gamma\left(^1S_0 \longrightarrow gg\right) = \frac{8\pi\alpha_s^2 |\Psi(0)|^2}{3m_q^2} \times \begin{cases} (1 + 4.8\alpha_s\pi) & \text{for } \eta_c \\ (1 + 4.4\alpha_s\pi) & \text{for } \eta_b. \end{cases} \quad (31)$$

The terms in the parenthesis refer to QCD corrections. The obtained results are given in Table 12.

4.5. M1 Transitions. M1 (magnetic dipole transition) decay widths can give more information about spin-singlet states. Moreover M1 transition rates show the validity of theory against experiment [11]. Magnetic transitions conserve both parity and orbital angular momentum of the initial and final states but in the M1 transitions the spin of the state changes. M1 width between two S-wave states is given by [51]

$$\Gamma\left(n^3S_1 \longrightarrow n'^1S_0 + \gamma\right) = \frac{4\alpha e_q^2 E_\gamma^3}{3m_q^2}\left(2J_f + 1\right)\left|\left\langle f\left|j_0\left(\frac{kr}{2}\right)\right|i\right\rangle\right|^2, \quad (32)$$

where $E_\gamma = (M_i^2 - M_f^2)/2M_i$ is the photon energy and $j_0(x)$ is the zeroth-order spherical Bessel function. In the case of small E_γ, spherical Bessel function $j_0(kr/2)$ tends to 1, $j_0(kr/2) \longrightarrow 1$. Thus transitions between the same principal quantum numbers, $n' = n$, are favored and usually known to be *allowed*. In the other case, when $n' \neq n$ the overlap integral between initial and final state is 0 and generally designated as *forbidden* transitions. The obtained transition rates for the allowed ones of S-wave charmonium and bottomonium states are given in Tables 13 and 14, respectively.

5. Results and Discussion

In the present paper we studied S-wave heavy quarkonium spectra with two phenomenological potentials. We have computed spin averaged masses, hyperfine splittings, Regge trajectories for pseudoscalar and vector mesons, decay constants, leptonic decay widths, two-photon and gluon decay widths, and allowed M1 partial widths of S-wave heavy quarkonium states.

In general, most of the quark model potentials tend to be similar, having a Coulomb term and a linear term. For example, in [11] they used standard color Coulomb plus linear scalar form, and also included a Gaussian smeared contact hyperfine interaction in the zeroth-order potential. In [13], the authors used a nonrelativistic potential model with screening effect. In [18] nonrelativistic linear potential and screened potential, in [14, 16, 44] a modified of nonrelativistic potential models and in [15] Hulthen potential are used. Potential models give reliable results with the appropriate parameters in the model. Therefore, the shape of the potential at the limits $r \longrightarrow 0$ and $r \longrightarrow \infty$ have similar behaviours.

Spin averaged mass spectra give idea about the formulation of model since the results are close to experimental values due to contributions from spin dependent interactions are small compared to contribution from potential part. If one ignores all spin dependent interactions, obtained results under this assumption are thought to be averages over related spin states for principal quantum number. Including hyperfine interaction, we obtained the mass spectra for pseudoscalar and vector mesons. The obtained spectra for both charmonium and bottomonium are in good agreement with the experimentally observed spectra and other theoretical studies.

Both power and logarithmic potentials produced approximately same mass differences and are in agreement with experiment for the lowest state in charmonium sector. But for the highest states, the shift is not compatible with the references. The reason for this should be the behaviour of linear part of the potential. In the case of bottomonium sector, mass differences of both power and logarithmic potentials are in accord with the given studies except the lowest state.

The fundamental point in the Regge trajectories is that they can predict masses of unobserved states. For the hadrons constituting of light quarks, the Regge trajectories are approximately linear but for the heavy quarkonium case Regge trajectories can be nonlinear. In the present work, we found that all Regge trajectories show nonlinear properties.

The decay constants are calculated for pseudoscalar and vector mesons by equating their field theoretical definition with the analogous quark model potential definition. This is valid in the nonrelativistic and weak binding limits where quark model state vectors form good representations of the Lorentz group [52, 53]. For pseudoscalar mesons, the corrected value of power and logarithmic potentials are a few MeV above than the available experimental data. For the rest of the pseudoscalar mesons, obtained results are compatible with other studies. In the case of vector mesons, logarithmic potential gave higher values than power potential. In the Υ meson, when the radially states are excited, both two potential gave similar results within the error of experimental value. Computations of the vector decay constant beyond the weak binding limit can be important in the quark potential model frame and need more elaboration [12].

Obtained leptonic decay widths are comparable with the experimental values and other theoretical studies. The QCD corrected factors are more close to experimental values for power and logarithmic potential and this can be referred as the importance of the QCD correction factor in calculating

Table 11: Two-photon decay widths (in keV). The widths calculated with and without QCD corrections are denoted by $\Gamma_{\gamma\gamma}$ and $\Gamma^0_{\gamma\gamma}$.

	Power		Logarithmic		[15]		[8]	[12]	Exp. [43]
State	$\Gamma^0_{\gamma\gamma}$	$\Gamma_{\gamma\gamma}$	$\Gamma^0_{\gamma\gamma}$	$\Gamma_{\gamma\gamma}$	$\Gamma^0_{\gamma\gamma}$	$\Gamma_{\gamma\gamma}$	$\Gamma_{\gamma\gamma}$	$\Gamma_{\gamma\gamma}$	
$\eta_c(1S)$	1.10	0.664	1.450	0.869	11.17	6.668	3.69	7.18	$7.2 \pm 0.7 \pm 0.2$
$\eta_c(2S)$	0.987	0.592	1.291	0.774	8.48	5.08	1.4	1.71	
$\eta_c(3S)$	0.907	0.543	1.184	0.710	7.57	4.53	0.930	1.21	
$\eta_c(4S)$	0.847	0.508	1.105	0.662			0.720		
$\eta_c(5S)$	0.801	0.480	1.044	0.620					
$\eta_b(1S)$	0.277	0.199	0.277	0.199	0.58	0.42	0.214	0.45	
$\eta_b(2S)$	0.212	0.153	0.246	0.177	0.29	0.20	0.121	0.11	
$\eta_b(3S)$	0.195	0.142	0.226	0.162	0.24	0.17	0.09	0.063	
$\eta_b(4S)$	0.188	0.136	0.211	0.151			0.07		
$\eta_b(5S)$	0.176	0.129	0.199	0.143					
$\eta_b(6S)$	0.164	0.116	0.182	0.134					

Table 12: Two-gluon decay widths (in MeV). The widths calculated with and without QCD corrections are denoted by Γ_{gg} and Γ^0_{gg}.

	Power		Logarithmic		[15]		[49]	Exp. [43]
State	Γ^0_{gg}	Γ_{gg}	Γ^0_{gg}	Γ_{gg}	Γ^0_{gg}	Γ_{gg}	Γ^0_{gg}	Γ_{gg}
$\eta_c(1S)$	32.04	50.15	41.93	32.44	50.82	66.68	15.70	26.7 ± 3.0
$\eta_c(2S)$	28.55	44.70	37.32	24.64	38.61	5.08	8.10	14 ± 7
$\eta_c(3S)$	26.22	41.04	34.23	53.59	21.99			
$\eta_c(4S)$	24.50	38.35	31.96	50.03				
$\eta_c(5S)$	23.15	36.24	30.18	47.24				
$\eta_b(1S)$	5.50	7.50	12.82	17.49	13.72	18.80	11.49	
$\eta_b(2S)$	4.90	6.69	11.41	15.56	6.73	9.22	5.16	
$\eta_b(3S)$	4.50	6.14	10.46	14.28	5.58	7.64	3.80	
$\eta_b(4S)$	4.20	5.74	9.77	13.33				
$\eta_b(5S)$	3.97	5.42	9.22	12.58				
$\eta_b(6S)$	3.62	5.18	8.68	10.86				

Table 13: Radiative M1 decay widths of charmonium. In [18] LP stands for linear potential and SP stands for screened potential.

Initial	Final	Power		Logarithmic		[15]	[18]		Exp. [43]
		E_γ (MeV)	Γ (keV)	E_γ (MeV)	Γ (keV)	Γ (keV)	Γ_{LP} (keV)	Γ_{SP} (keV)	Γ (keV)
J/ψ	$\eta_c(1S)$	114.9	1.96	113.8	2.83	3.28	2.39	2.44	1.13 ± 0.35
$\psi(2S)$	$\eta_c(2S)$	111.5	1.39	101.5	2.01	1.45	0.19	0.19	
$\psi(3S)$	$\eta_c(3S)$	93.8	1.10	93.8	1.59		0.051	0.088	
$\psi(4S)$	$\eta_c(4S)$	87.1	0.88	87.1	1.27				
$\psi(5S)$	$\eta_c(5S)$	83.2	0.74	83.2	1.10				

Table 14: Radiative M1 decay widths of bottomonium.

Initial	Final	Power		Logarithmic		[10]	[44]	[16]	Exp. [43]
		E_γ (MeV)	Γ (eV)	E_γ (MeV)	Γ (eV)	Γ (eV)	Γ (eV)	Γ (eV)	Γ (eV)
$\Upsilon(1S)$	$\eta_b(1S)$	27.9	0.88	31.9	1.46	5.8	10	9.34	
$\Upsilon(2S)$	$\eta_b(2S)$	24.9	0.62	28.9	1.09	1.4	0.59	0.58	
$\Upsilon(3S)$	$\eta_b(3S)$	25.9	0.54	25.9	0.78	0.8	0.25	0.66	
$\Upsilon(4S)$	$\eta_b(4S)$	20.9	0.37	20.9	0.41				
$\Upsilon(5S)$	$\eta_b(5S)$	19.9	0.32	19.9	0.35				
$\Upsilon(6S)$	$\eta_b(6S)$	14.3	0.29	14.4	0.27				

Table 15: Exotic states. Experimental data are taken from [43] unless stated. The units for mass and strong decays are in MeV and two-photon decay is in keV.

	Mass			Strong decay			Two-photon decay		
	Power	Logarithmic	Experiment	Power	Logarithmic	Experiment	Power	Logarithmic	Experiment
$X(3940)$			$3942^{+7}_{-6} \pm 6$			$37^{+26}_{-15} \pm 8$			
$\eta_c(3S)$	3983	3887		41.04	53.59		0.543	0.710	
$X(4160)$			4191 ± 5			70 ± 10			0.48 ± 0.22 [50]
$\eta_c(4S)$	4240	4117		38.35	50.03		0.508	0.612	
$\psi(4415)$			4421 ± 4			62 ± 20			0.58 ± 0.07
$\eta_c(5S)$	4441	4297		36.24	47.24		0.480	0.620	

the decay constants and other short range phenomena using potential models.

$^1S_0$ levels of charmonium and bottomonium states can decay into two photons or gluons. Especially two- photon decays of these levels are important for understanding the accuracy of theoretical models. Obtained results are smaller than the nonrelativistic widths including the one-loop QCD correction factor. For example, results of power and logarithmic potentials in $\eta_c(1S)$ are not in accord with experimental data. The reason of these differences can be due to the static potential between quarks that we used in the solution of two-body Schrödinger equation. For higher states, power and logarithmic potentials results are comparable with other studies. Two-photon decays are complicated processes such as pseudoscalar meson decay to two photons is governed by an intermediate vector meson followed by a meson dominance transition to a photon [12]. These schematic diagrams must be added to calculations to obtain a whole picture. For two-gluon decay widths, two phenomenological potentials gave comparable results with the available experimental data. Notice that in some cases QCD corrected factor is in accord with the experimental data whereas in some cases it is not. The reason for this can be that, there are significant radiative corrections from three-gluon decays so computing only two-gluon decay width could not explain the mechanism in all details.

Finally M1 transitions are calculated. The M1 radiative decay rates are very sensitive to relativistic effects. Even for allowed transitions relativistic and nonrelativistic results differ significantly. An important example is the decay of $J/\psi \longrightarrow \eta_c\gamma$. The nonrelativistic predictions for its rate are more than two times larger than the experimental data [10]. In the charmonium sector, the available experimental data for $J/\psi \longrightarrow \eta_c(1S)$ is comparable with the power potential result, while logarithmic potential result is 1 eV higher. In the bottomonium sector, there is no experimental data available on M1 transitions. Since photon energies and transition rates are very small, the detection of these transitions is an objection. And this can be a reason why no spin-singlet S-wave levels $\eta_b(n^1S_0)$ have been observed yet [10]. The obtained values for M1 transitions are comparable with the references.

Some states in the charmonium and bottomonium sector show properties different from the conventional quarkonium state. Some examples are $X(3940)$, $X(4160)$, and $\psi(4415)$. For $X(3940)$, there is not much available experimental data and more is needed. Wang et al. studied two-body open charm OZI-allowed strong decays of $X(3940)$ and $X(4160)$ considered as $\eta_c(3S)$ and $\eta_c(4S)$, respectively, by the improved Bethe-Salpeter method combined with the $^3P_0$ [54]. They calculated strong decay width of $X(3940)$ as $\Gamma = (33.5^{+18.4}_{-15.3})$ MeV and $X(4160)$ as $\Gamma = (69.9^{+22.4}_{-21.1})$ MeV where the experimental values are $\Gamma = (37^{+26}_{-15} \pm 8)$ MeV for $X(3940)$ and $\Gamma = (70 \pm 10)$ MeV for $X(4160)$ [43]. They concluded that $\eta_c(3S)$ is a good candidate of $X(3940)$ and $\eta_c(4S)$ is a not good candidate of $X(4160)$ due to larger decay width of $\Gamma(D\overline{D}^*)/\Gamma(D^*\overline{D}^*)$ comparing to experimental data. We give our results comparing to these exotic states in Table 15.

Looking at Table 15, we can deduce that, according to our model and results, we can assign $X(3940)$ as $\eta_c(3S)$, $X(4160)$ as $\eta_c(4S)$, and $\psi(4415)$ as $\eta_c(5S)$. To be more accurate, more data is needed to corroborate whether these states are conventional quarkonium or not.

6. Conclusions

Quark potential models have been very successful to study on various properties of mesons. The short distance behaviour of interquark potential appears to be similar where QCD perturbation theory can be applied where at large distance the potential is linear in r where nonperturbative methods are need to be used. The improvements on the potentials can be made and spin-spin, spin-orbit type interactions can be added to model to arrive high accuracy. The potential model approach is a valuable task, which has given to us many insights into the nature of both heavy and light quarkonium physics. Using a relativistic approach together with a model in which $B\overline{B}$ and $D\overline{D}$ thresholds are taken into account, detailed analysis can be made on various aspects of heavy quarkonium.

Data Availability

No data were used to support this study.

Conflicts of Interest

The author declares that they have no conflicts of interest.

References

[1] T. Kawanai and S. Sasaki, "Charmonium potential from full lattice QCD," *Physical Review D: Particles, Fields, Gravitation and Cosmology*, vol. 85, no. 9, 2012.

[2] A. Le Yaouanc, L. Oliver, O. Pène, and J. C. Raynal, "Spontaneous breaking of chiral symmetry for confining potentials," *Physical Review D: Particles, Fields, Gravitation and Cosmology*, vol. 29, no. 6, pp. 1233–1257, 1984.

[3] S. Bolognesi, K. Konishi, M. Shifman, and D. Phys. Rev, "Patterns of symmetry breaking in chiral QCD," *Physical Review D, Covering Particles, Fields, Gravitation, and Cosmology*, vol. 97, no. 9, Article ID 094007, 2018.

[4] T. Appelquist and H. D. Politzer, " Heavy Quarks and ," *Physical Review Letters*, vol. 34, no. 1, pp. 43–45, 1975.

[5] A. De Rújula and S. L. Glashow, "Is bound charm found?" *Physical Review Letters*, vol. 34, no. 1, pp. 46–49, 1975.

[6] E. Eichten, K. Gottfried, T. Kinoshita, K. D. Lane, and T. M. Yan, "Interplay of confinement and decay in the spectrum of charmonium," *Physical Review Letters*, vol. 36, p. 500, 1976.

[7] D. P. Stanley and D. Robson, "Nonperturbative potential model for light and heavy quark-antiquark systems," *Physical Review D: Particles, Fields, Gravitation and Cosmology*, vol. 21, no. 11, pp. 3180–3196, 1980.

[8] S. Godfrey and N. Isgur, "Mesons in a relativized quark model with chromodynamics," *Physical Review D: Particles, Fields, Gravitation and Cosmology*, vol. 32, no. 1, pp. 189–231, 1985.

[9] L. P. Fulcher, "Matrix representation of the nonlocal kinetic energy operator, the spinless Salpeter equation and the Cornell potential," *Physical Review D*, vol. 50, p. 447, 1994.

[10] D. Ebert, R. N. Faustov, and V. O. Galkin, " Properties of heavy quarkonia and ," *Physical Review D: Particles, Fields, Gravitation and Cosmology*, vol. 67, no. 1, 2003.

[11] T. Barnes, S. Godfrey, and E. S. Swanson, "Higher charmonia," *Physical Review D: Particles, Fields, Gravitation and Cosmology*, vol. 72, article 054026, 2005.

[12] O. Lakhina and E. S. Swanson, "Dynamic properties of charmonium," *Physical Review D*, vol. 74, 2006.

[13] B. Q. Li and K. T. Chao, "Higher charmonia and X, Y, Z states with screened potential," *Physical Review D: Particles, Fields, Gravitation and Cosmology*, vol. 79, Article ID 013011, 2009.

[14] B. Q. Li and K. T. Chao, "Bottomonium Spectrum with Screened Potential," *Communications in Theoretical Physics*, vol. 52, pp. 653–661, 2009.

[15] K. B. V. K. Bhaghyesh and A. P. Monteiro, "Heavy quarkonium spectra and its decays in a nonrelativistic model with Hulthen potential," *Journal of Physics G: Nuclear and Particle Physics*, vol. 38, Article ID 085001, 2011.

[16] J. Segovia, P. G. Ortega, D. R. Entem, and F. Fernandez, "Bottomonium spectrum revisited," *Physical Review D*, vol. 93, 2016.

[17] S. Godfrey, K. Moats, and E. S. Swanson, "B and B_s meson spectroscopy," *Physical Review D: Particles, Fields, Gravitation and Cosmology*, vol. 94, no. 5, 2016.

[18] W.-J. Deng, H. Liu, L.-C. Gui, and X.-H. Zhong, "Spectrum and electromagnetic transitions of bottomonium," *Physical Review D: Particles, Fields, Gravitation and Cosmology*, vol. 95, Article ID 074002, 2017.

[19] D. B. Lichtenberg, "Excited quark production at Hadron colliders," *International Journal of Modern Physics A*, vol. 2, no. 6, pp. 1669–1705, 1987.

[20] N. Brambilla, *Quarkonium Working Group*, CERN Yellow Report, 2005, arXiv:hep-ph/0412158.

[21] E. Eichten, K. Gottfried, T. Kinoshita, J. Kogut, K. D. Lane, and T.-M. Yan, "Spectrum of charmed quark-antiquark bound states," *Physical Review Letters*, vol. 34, no. 6, pp. 369–372, 1975.

[22] J. Richardson, "The heavy quark potential and the Υ, J/ψ systems," *Physics Letters B*, vol. 82B, p. 272, 1979.

[23] Y.-Q. Chen and Y.-P. Kuang, "Improved QCD-motivated heavy-quark potentials with explicit Λ_{MS} dependence," *Physical Review D*, vol. 46, p. 1165, 1992.

[24] Y.-Q. Chen and Y.-P. Kuang, "Erratum: "Improved QCD-motivated heavy-quark potentials with explicit Λ_{MS} dependence"," *Physical Review D: Particles, Fields, Gravitation and Cosmology*, vol. 47, p. 35, 1993.

[25] V. Khruschev, V. Savrin, and S. Semenov, "On the parameters of the QCD-motivated potential in the relativistic independent quark model," *Physics Letters B*, vol. 525, no. 3-4, pp. 283–288, 2002.

[26] A. Martin, "A simultaneous fit of bb, cc, ss (bcs Pairs) and cs spectra," *Physics Letters B*, vol. 100, p. 511, 1981.

[27] M. Machacek and Y. Tomozawa, "ψ Phenomenology and the nature of quark confinement," *Annals of Physics*, vol. 110, p. 407, 1978.

[28] G. Fogleman, D. B. Lichtenberg, and J. G. Wills, "Heavy-meson spectra calculated with a one-parameter potential," *Lettere al Nuovo Cimento*, vol. 26, p. 369, 1979.

[29] C. Quigg and J. L. Rosner, "Quantum mechanics with applications to quarkonium," *Physics Reports*, vol. 56, no. 4, pp. 167–235, 1979.

[30] C. Quigg and J. L. Rosner, "Quarkonium level spacings," *Physics Letters B*, vol. 71B, pp. 153–157, 1977.

[31] S. Xiaotong and L. Hefen, "A new phenomenological potential for heavy quarkonium," *Zeitschrift für Physik C Particles and Fields*, vol. 34, no. 2, pp. 223–231, 1987.

[32] C. Quigg, H. B. Thacker, and J. L. Rosner, "Constructive evidence for flavor independence of the quark-antiquark potential," *Physical Review D: Particles, Fields, Gravitation and Cosmology*, vol. 21, Article ID 3393, p. 234, 1980.

[33] W. Buchmüller, Y. Jack Ng, and S.-H. H. Tye, "Hyperfine splittings in heavy-quark systems," *Physical Review D: Particles, Fields, Gravitation and Cosmology*, vol. 24, no. 12, pp. 3312–3314, 1981.

[34] C. Bachas, "Concavity of the quarkonium potential," *Physical Review D: Particles, Fields, Gravitation and Cosmology*, vol. 33, no. 9, pp. 2723–2725, 1986.

[35] S. K. Choi, "Belle collaboration," *Physical Review Letters*, vol. 91, Article ID 262001, 2003.

[36] X.-W. Kang and J. A. Oller, "Different pole structures in line shapes of the X(3872)," *The European Physical Journal C*, vol. 77, no. 6, 2017.

[37] R. R. Horgan, "The construction and classification of wavefunctions for the harmonic oscillator model of three quarks," *Journal of Physics G: Nuclear Physics*, vol. 2, p. 625, 1976.

[38] N. Isgur and G. Karl, "P-wave baryons in the quark model," *Physical Review D: Particles, Fields, Gravitation and Cosmology*, vol. 18, no. 11, pp. 4187–4205, 1978.

[39] A. W. Hendry, "Decays of high spin Δ^* and N^* resonances in the quark model," *Annals of Physics*, vol. 140, no. 65, 1982.

[40] A. W. Hendry and D. B. Lichtenberg, "Properties of hadrons in the quark model," *Fortschritte der Physik/Progress of Physics banner*, vol. 33, no. 3, pp. 139–231, 1985.

[41] K. B. V. Kumar, B. Hanumaiah, and S. Pepin, "Meson spectrum in a relativistic harmonic model with instanton-induced interaction," *The European Physical Journal A - Hadrons and Nuclei*, vol. 19, no. 9, p. 247, 2004.

[42] K. B. V. Kumar, M. Y.-L. Bhavyashri, and A. P. Monteiro, "P-wave meson spectrum in a relativistic model with instanton induced interaction," *International Journal of Modern Physics A*, vol. 24, 2009.

[43] M. Tanabashi, "Particle Data Group," *Physical Review D: Particles, Fields, Gravitation and Cosmology*, vol. 98, Article ID 030001, 2018.

[44] S. Godfrey and K. Moats, " Erratum: ," *Physical Review D: Particles, Fields, Gravitation and Cosmology*, vol. 92, no. 11, 2015.

[45] V. Lengyel, Y. Fekete, I. Haysak, and A. Shpenik, "Calculation of hyperfine splitting in mesons using configuration interaction approach," *The European Physical Journal C*, vol. 21, no. 2, pp. 355–359, 2001.

[46] R. Van Royen and V. F. Weisskopf, "Protsyessy raspada adronov i modyel cyrillic small soft sign kvarkov," *Il Nuovo Cimento A*, vol. 50, no. 3, pp. 617–645, 1967.

[47] E. Braaten and S. Fleming, "QCD radiative corrections to the leptonic decay rate of the B_c meson," *Physical Review D*, vol. 52, p. 181, 1995.

[48] W. Kwong, P. B. Mackenzie, R. Rosenfeld, and J. L. Rosner, "Quarkonium annihilation rates," *Physical Review D: Particles, Fields, Gravitation and Cosmology*, vol. 37, no. 11, pp. 3210–3215, 1988.

[49] J. T. Laverty, S. F. Radford, and W. W. Repko, "\ga\ga and g g decay rates for equal mass heavy quarkonia," *High Energy Physics - Phenomenology*, 2009, arXiv:hep-ph/0901.3917v3.

[50] M. Ablikim, J. Z. Bai, Y. Ban, X. Cai, H. F. Chen, and H. S. Chen, "Determination of the $\psi(3770)$, $\psi(4040)$, $\psi(4160)$ and $\psi(4415)$ resonance parameters," *Physics Letters B*, vol. 660, no. 3, pp. 315–319, 2008.

[51] E. Eichten, K. Gottfried, T. Kinoshita, K. D. Lane, and T. -. Yan, "Charmonium: The model," *Physical Review D: Particles, Fields, Gravitation and Cosmology*, vol. 17, no. 11, pp. 3090–3117, 1978.

[52] C. Hayne and N. Isgur, "Beyond the wave function at the origin: Some momentum-dependent effects in the nonrelativistic quark model," *Physical Review D: Particles, Fields, Gravitation and Cosmology*, vol. 25, no. 7, pp. 1944–1950, 1982.

[53] N. Isgur, D. Scora, B. Grinstein, and M. B. Wise, "Semileptonic *B* and *D* decays in the quark model," *Physical Review D: Particles, Fields, Gravitation and Cosmology*, vol. 39, no. 3, pp. 799–818, 1989.

[54] Z.-H. Wang, Y. Zhang, L.-B. Jiang, T.-H. Wang, Y. Jiang, and G.-L. Wang, "The strong decays of X(3940) and X(4160)," *European Physical Journal C*, vol. 77, no. 1, article 43, 2017.